ACS Applies Materials and Interfaces Volume 11, Issue 37, 2019, pp. 34497–34506
DOI:10.1021/acsami.9b12946

Modulating electrode kinetics for discrimination of dopamine by PEDOT:COOH interface doped with negatively-charged tri-carboxylate

Lingyin Meng[1], Anthony P.F. Turner[1], Wing Cheung Mak[1*]

[1]Biosensors and Bioelectronics Centre, Division of Sensor and Actuator Systems, Department of Physics, Chemistry and Biology, Linköping University, SE-581 83 Linköping, Sweden

[*]Corresponding author. E-mail address: wing.cheung.mak@liu.se (W.C. Mak).

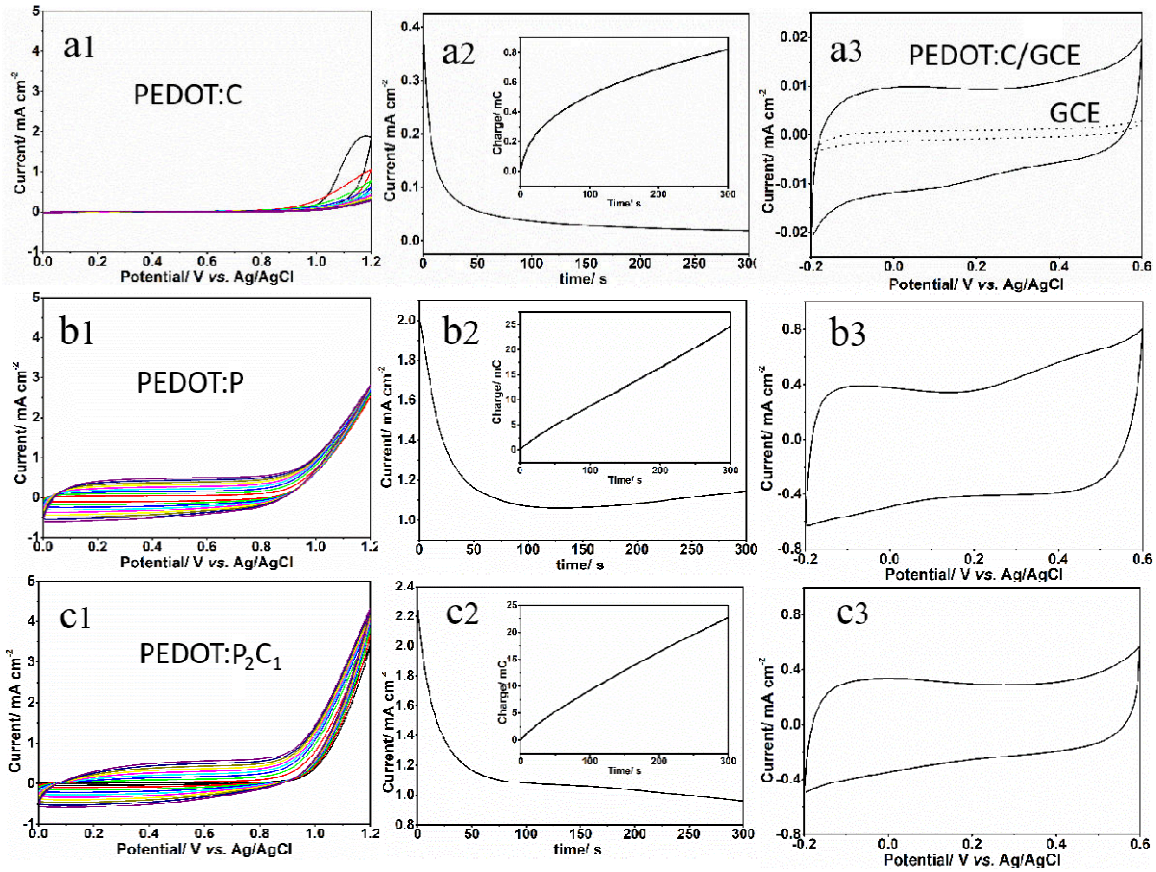

Figure S1. Cyclic voltammetry (CVs) and Chronoamperometry (CA) electropolymerization of PEDOT by 10 mM EDOT with 20 mM citrate (a1-2), 20 mM $LiClO_4$ (b1-2), 10 mM citrate and 20 mM $LiClO_4$ (c1-2) as dopant and supporting electrolyte; inset of a2, b2 c2 are the corresponding charge of CA electropolymerization. CVs of CA-electropolymerised PEDOT:C

(a3), PEDOT:P (b3) and PEDOT:P_2C_1 (c3) in 0.1 M PBS (pH=7.4) with scan rate of 50 mV s^{-1}.

Figure S1 a1 and b1 show the CVs electropolymerization of 10 mM EDOT with 20 mM citrate (a) and $LiClO_4$ (b) as dopant and supporting electrolyte on GCE. It can be observed from a1 that the onset oxidation potential for EDOT is around 1.0 V, but the current at the range of 0-1.0 V demonstrated no apparent increase with the increasing of CV cycles. On the contrary, in the 20 mM $LiClO_4$ solution, the onset oxidation potential for EDOT decreased to 0.9 V in the first forward scan (b1) and current crossover at about 0.85 V in the reverse scan for beginning of characteristic nucleation process[1]. And upon successive cycles, the current showed notable increase, implying successful growth process of PEDOT on the electrode surface. Chronoamperometry (CA) was further used as an alternative technique for PEDOT electropolymerisation at 1.1 V for 300 s and the corresponding current-time curves were shown in a2 and b2. For PEDOT:C, the initial current is ascribed to the charging of double layer, followed by the fast decrease of current to around 0.019 mA cm^{-2} with the final deposition charge of 0.86 mC. The initial charging of PEDOT:P is much higher than that of PEDOT:C and decayed more slowly due to the effectively faradaic processes occurring at the electrode surface, with remained current of 1.15 mA cm^{-2} at the end. The deposition charge of PEDOT:P (24.55 mC) is 28.5 times higher than that of PEDOT:C. The obvious difference between $LiClO_4$ and citrate may be explained by anion mobility due to the higher doping affinity of ClO_4^- as a counterion compared to citrate. During the electropolymerization process, polaron-anion ionic pairs formed and were trapped in the polymer matrix. The more mobile anions (ClO_4^-) will be replaced by monomer molecules in a faster way than that of slower ones (citrate)[1]. Therefore, increasing currents were observed for the following scans with increased amount of PEDOT electropolymerization. The CA-electropolymerised PEDOT:C and PEDOT:P electrodes were also tested in 0.1 M PBS (pH=7.4) by CVs. The PEDOT:C electrode (a3) showed quite small capacitance rectangular box that is slightly higher than bare GCE (dash curve in a3), while PEDOT:P electrode possessed more than 38 times broader background in b3. All the results certified the non-effective electropolymerisation efficiency of PEDOT by citrate on the

electrode surface compared to $LiClO_4$. Taking 10 mM citrate and 20 mM $LiClO_4$ as dopant and supporting electrolyte, the CVs and CV electropolymerization showed similar trend to $LiClO_4$ with increased electropolymerization efficiency compared to citrate. The deposition charge of PEDOT:P_2C_1 is 23.60 mC, which is slightly lower than PEDOT:P and 27.4 times higher than PEDOT:C.

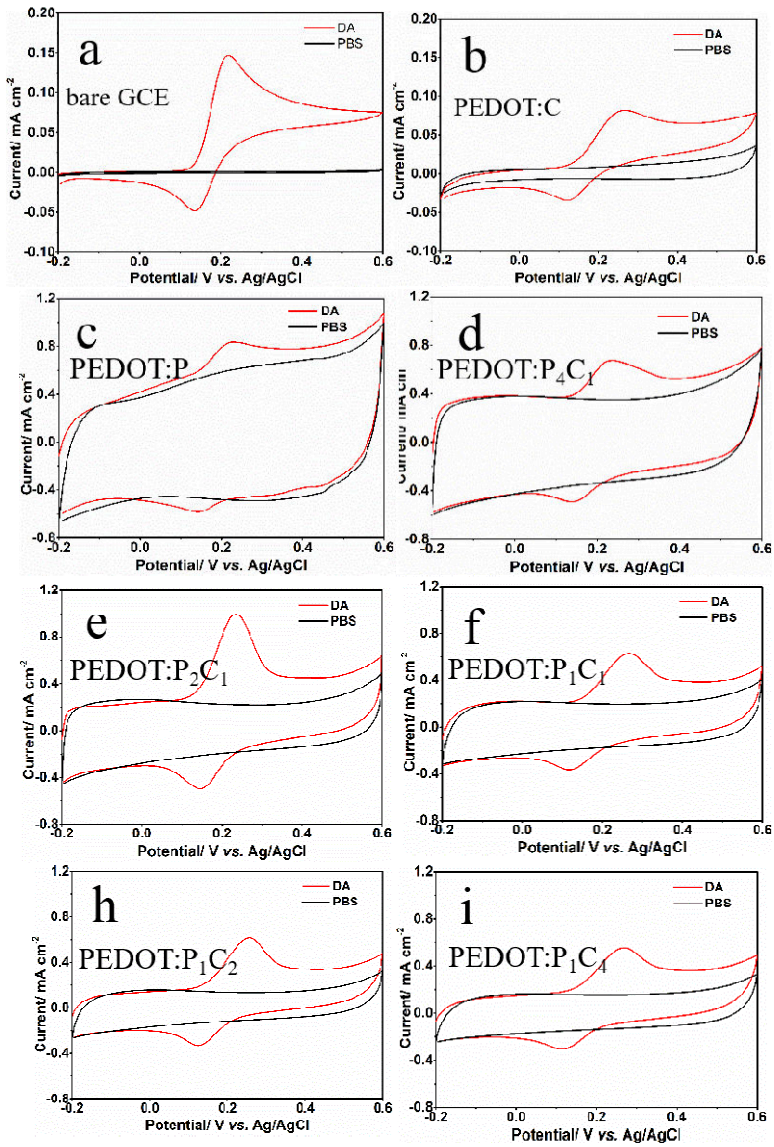

Figure S2. CVs bare GCE (a), PEDOT:C (b), PEDOT:P (c), PEDOT:P_4C_1 (d), PEDOT:P_2C_1 (e) PEDOT:P_1C_1 (f), PEDOT:P_1C_2 (h), and PEDOT:P_1C_4 (i), respectively without (black curve) and with 0.5 mM DA in 0.1 M PBS (pH 7.4) with scan rate of 50 mV s^{-1}.

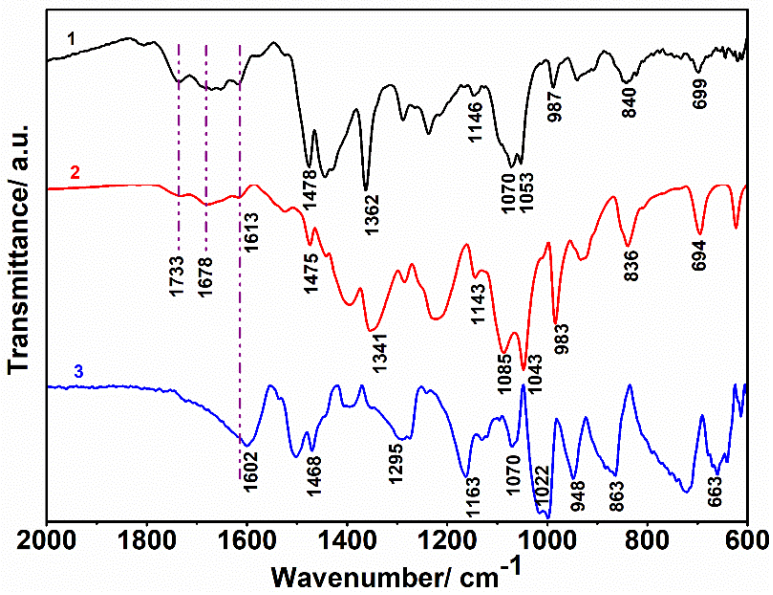

Figure S3. FTIR spectra of PEDOT:C (1), PEDOT:P_2C_1 (2) and PEDOT:P (3).

FTIR spectra were used to characterize the doping effect of citrate and $LiClO_4$ on the PEDOT films. On the whole, the PEDOT:P_2C_1 spectrum (curve 2) shows the shape similar to PEDOT:C (curve 2) and shifted peak positions as PEDOT:P (curve 3) spectrum, which may be caused by the co-doping effect from citrate and ClO_4^-. As shown in PEDOT:C (curve 1) and PEDOT:P2C1 (curve 2) spectra in the Fig. S3, the bands at bands at 1733 and 1678 cm^{-1} were assigned to C=O stretching of the COOH group[2-4], suggesting the successful doping of ternary citrate into the PEDOT films. The bands at 1613 cm^{-1} for PEDOT:C and PEDOT:P_2C_1 spectra are considered to be the characteristic peak of the PEDOT-doped state, while the band at PEDOT:P spectrum shifted to around 1602 cm^{-1}. For PEDOT:C , the C=C and C-C stretching in the thiophene moiety appear at 1478 and 1632 cm^{-1}.[5-6] The bands at 1146, 1070, 1053 cm^{-1} are ascribed to the C-O-C stretching in the ethylenedioxy group, while the bands at 987, 840 and 699 are attributed to the C-S bond stretching.[7] Compared to the PEDOT:C, PEDOT:P_2C_1 demonstrates the same bands with small shift. For the thiophene ring, the C=C and C-C stretching are located at 1475 and 1431 cm^{-1}, while C-S bond stretching are at 983, 836 and 694 cm^{-1}. And for the ethylenedioxy ring, the C-O-C stretching bands are at 1143, 1085 and 1043 cm^{-1}. The PEDOT:P shows the typically electropolymerized PEDOT spectrum with the C=C

and C-C stretching at 1468 and 1295 cm^{-1}, and C-S bond stretching at 948, 863 and 663 cm^{-1}, while C-O-C stretching bands at 1163, 1070 and 1022 cm^{-1}.

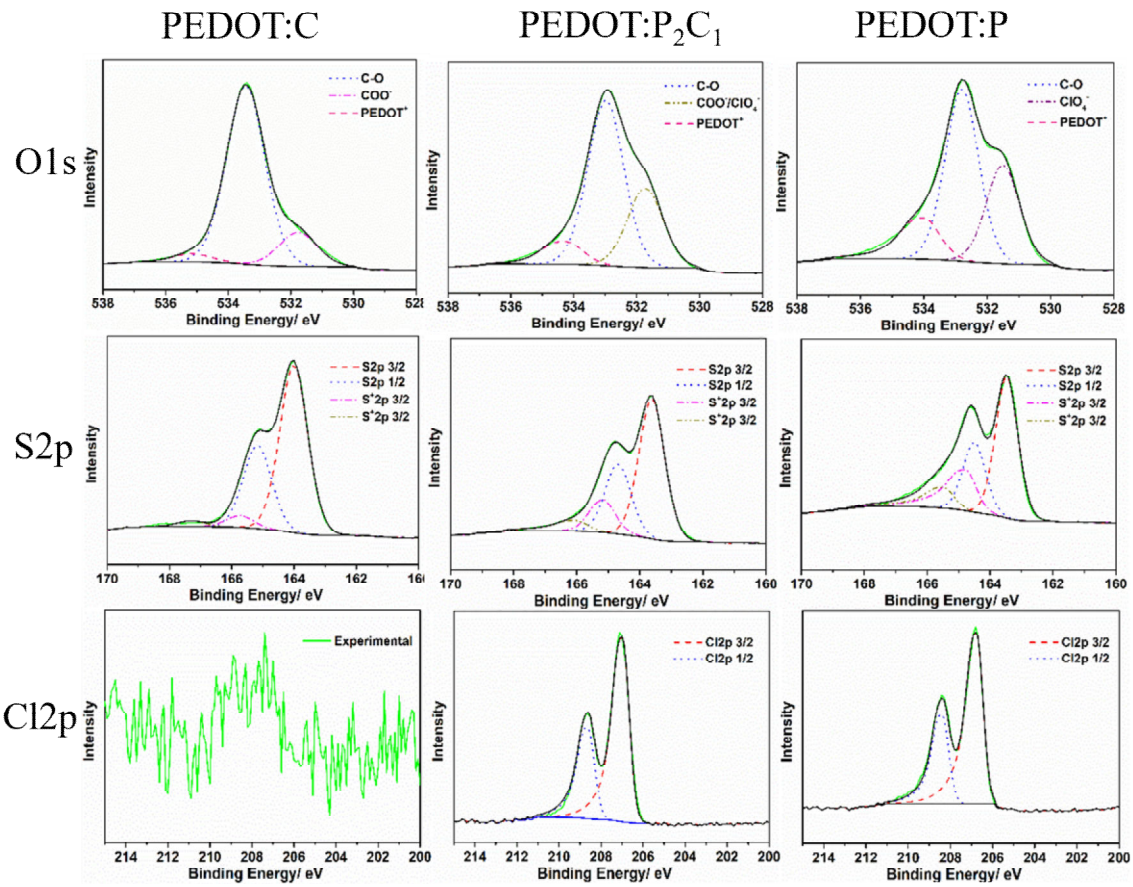

Figure S4. High resolution XPS spectra of O1s, S2p and Cl2p core-level for PEDOT:C, PEDOT:P and PEDOT:P_2C_1.

O1s: The characteristic C-O bonding was present as main peaks in PEDOT:C (533.4 eV), PEDOT:P_2C_1 (533.0 eV) and PEDOT:P (532.7 eV). The smaller peaks at 535.2 eV (PEDOT:C), 534.3 eV (PEDOT:P_2C_1) and 534.0 eV (PEDOT:P) are ascribed to the doped state $PEDOT^+$.[8] The peaks at 531.8 in PEDOT:C and 531.5 eV in PEDOT:P are assigned to citrate and ClO_4^-, respectively. In PEDOT:P_2C_1, the peak at 531.7 eV can be assigned to the co-contribution of citrate and ClO_4^-.

S2P: The main sulfur spin-split peaks (S2p 3/2 and S2p 3/2) with a separation of 1.1 eV are assigned for the S in PEDOT ring for all these three PEDOT interfaces[9-10]. The other pair of doublet peaks at high binding energy originate from the positively charged sulfur in the thiophene moiety due to the π-electrons delocalization.[8, 10]

Cl2p: For PEDOT:C , there is no Cl2p peaks. In PEDOT:P and PEDOT:P_2C_1, the Cl 2p spectra show the ClO_4^- characteristic spin-split peaks with a 1.6 eV separation. And they have an asymmetric tail to the high binding energy sites because of ClO_4^- charging effects by the positively charged sulfur within the thiophene ring.[10]

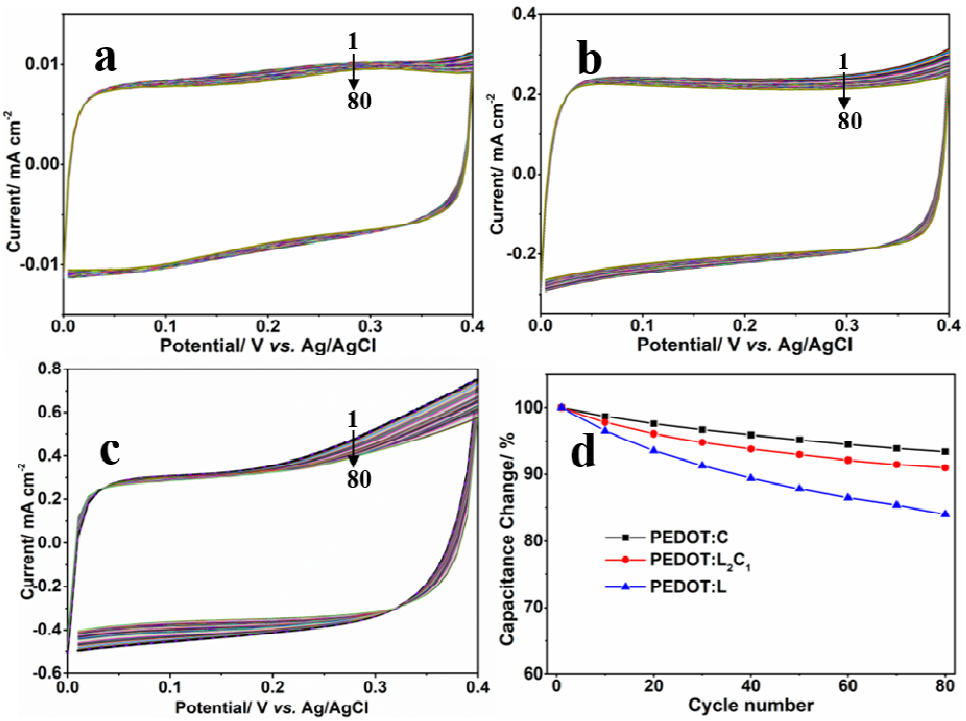

Figure S5. Stability test from CVs of PEDOT:C (a), PEDOT:P_2C_1 (b) and PEDOT:P (c) in PBS (0.1 M, pH 7.4) at a scan rate of 50 mV s^{-1}. (d) the capacitance changes of different PEDOT electrodes quantified by CV curves in the range of 0-0.4 V.

The stability of the PEDOT-modified electrodes were tested by observing the CVs in PBS (0.1 M, pH 7.4) over range of 0-0.4 V. As shown in Figure 5S, the PEDOT:C (a), PEDOT:P_2C_1 (b) and PEDOT:P (c) showed slightly decreased current with increase of cycling numbers. The charge capacitance for different PEDOT electrodes was calculated from the CVs to evaluate the stability of PEDOT in Figure 5S d. After 80 cycles, the PEDOT:C electrode remained at 93.4 % of its initial capacitance value, implying good stability of PEDOT doped with citrate. However, for the PEDOT:P, the capacitance was only able to retain 84.0 % of the initial value. That can be ascribed to the gradual leakage of ClO_4^- from PEDOT matrix. Compared to that of PEDOT:P,

the PEDOT:P_2C_1 electrodes showed improved stability with 91.0 % of its initial value remaining. The increased cycling stability and decreased leakage of dopant (citrate) from the PEDOT matrix may be caused by the higher doping stability due to the tri-carboxylic acid groups compared to the small dopant ClO_4^-.

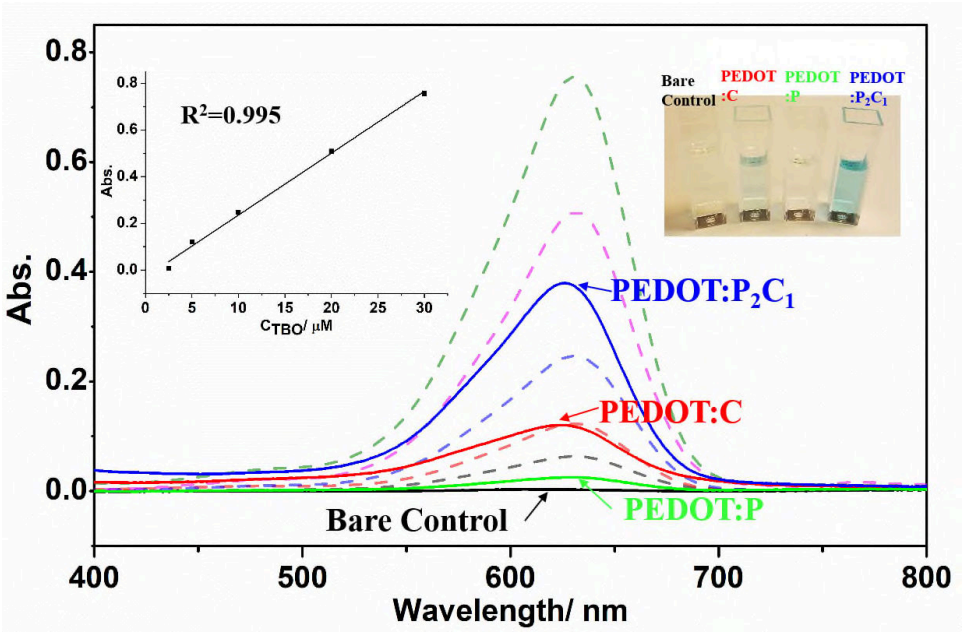

Figure S6. Absorbance spectra of TBO standard solution from 2.5-30 μM (dash line) and dissolved dye solution for bare substrate control, PEDOT:C, PEDOT:P and PEDOT:P2C1 electrodes, left inset is the corresponding calibration curve for TBO concentration *vs.* Absorbance (Regression equation: A=0.02652C-0.03056, R^2=0.995), right inset is the digital photos of dissolved dye solution for different PEDOT electrodes.

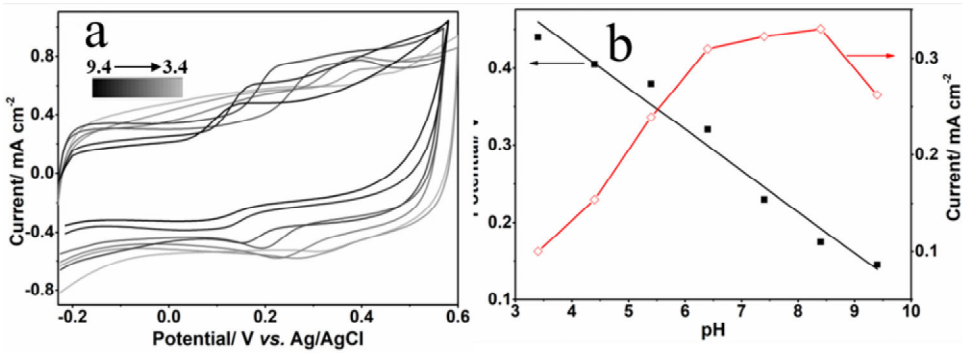

Figure S7. (a) CVs response of 0.5 mM DA at PEDOT:P interface in 0.1 M PBS with various pH ranging 3.4-9.4; (b) (d) corresponding plots of peak potential and current density *vs* pH. Scan rate 50 mV s^{-1}.

The peak potential shifted negatively with the pH increase, indicating that the electroactivity of DA is pH dependent. And the oxidation peak potentials towards DA at the PEDOT:P were linearly proportional to pH according to the equation: E_{pa} = 0.641-0.053 pH (R^2 = 0.969). The slope of -0.053 V/pH is close to the theoretical value of -0.059 V/pH. The oxidation current density increased gradually with increase of pH, and reached the highest peak current density at 8.4, then decreased after 8.4.

Table S1. Fitted parameters obtained by EIS spectra of PEDOT:P2C1 and PEDOT:P in 0.1 M PBS (pH 7.4) without and with 0.5 mM AA, 0.5 mM DA and 0.5 mM UA at their corresponding oxidation peak potential.

	Potential (V)	**System**	**Rs (Ω)**	**Rct (kΩ)**	**Rct change[a] (%)**	**W (Ω $s^{-1/2}$)**	**W change[b] (%)**	**Q (S s^{n})**	**n**
PEDOT:P2C1	0.240	PBS	153	439	66.7	0.0339	142.2	0.383	0.986
		PBS+DA	140	146		0.0821		0.452	0.919
	0.190	PBS	189	524	26.7	0.0503	54.7	0.368	0.971
		PBS+AA	180	384		0.0778		0.359	0.968
	0.350	PBS	151	485	29.3	0.0502	38.4	0.363	0.941
		PBS+UA	145	343		0.0695		0.353	0.938
PEDOT:P	0.240	PBS	182	485	46.4	0.0414	68.8	0.689	0.947
		PBS+DA	177	260		0.0699		0.647	0.892
	0.030	PBS	160	653	76.1	0.0528	51.5	0.470	0.928
		PBS+AA	147	156		0.0800		0.447	0.856
	0.345	PBS	191	497	66.2	0.0433	125	0.625	0.954
		PBS+UA	172	168		0.0975		0.600	0.950

Note: [a]Rct Change=[$Rct_{(PBS)}$ - $Rct_{(PBS+analyte)}$]/$Rct_{(PBS)}$×100%; [b]W change=[$W_{(PBS+analyte)}$ - $W_{(PBS)}$]/$W_{(PBS)}$×100%

Electrochemical impedance spectroscopy (EIS) measurements were carried out at PEDOT electrodes in 0.1 M PBS (pH=7.4) in the presence/absence of different analytes (DA, AA or UA, 0.5 mM) with a frequency range of 0.01 Hz to 100 kHz, 5 mV amplitude, and corresponding oxidation peak potential for different analytes. The impedance spectra were then fitted to an equivalent electrical circuit via ZSimpWin Software (AMETEK Scientific instruments), in which Rs is the solution resistance, RCT is charge transfer resistance as a measure of electrode reaction kinetics, W is generalized finite Warburg element corresponding to the diffusion contribution, Q is the constant phase element, n is the fitted exponent factor.11-14

Table S2. Comparison of the determination of DA at various PEDOT modified electrodes

Electrode	Technique	Linear range (μM)	Sensitivity ($\mu A\ \mu M^{-1}$)	Detection limit (μM)	Reference
PEDOT/CNT/CPE	DPV	0.1-20	-	0.02	Xu[15]
PEDOT/ionic liquid/GCE	Amperometry	0.2-312	0.04535	0.051	Ge[16]
PEDOT/Pd/GCE	DPV	0.5-1	1.9	0.5	Harish[17]
PEDOT/Pd/rGO/GCE	DPV	1-200	0.0213	0.14	Choe[18]
PEDOT/Ni/Si/MCP	DPV	12-48	0.0054 ($\mu A\ cm^{-2}\ \mu M^{-1}$)	1.5	Yu[19]
PEDOT/NF/CD/Au	DPV	2-320	0.1191	0.003	Atta[20]
PEDOT/SDS/Pt	LSV	0.5-25, 30-100	-	0.061, 0.086	Atta[21]
PEDOT:P/GCE	DPV	5-85	0.0550 (0.778 $\mu A\ cm^{-2}\ mM^{-1}$)	1.25	This work
PEDOT:P_2C_1/GCE	DPV	1-85	0.228 (0.00324 $\mu A\ cm^{-2}\ \mu M^{-1}$)	0.15	This work

Note. CNT: carbon nanotube; CPE: carbon paste electrode; MCP: microchannel plate; NF: Nafion; CD: β-cyclodextrin; SDS: sodium dodecyl sulfate.

1. Melato, A.; Mendonça, M.; Abrantes, L., Effect of the electropolymerisation conditions on the electrochemical, morphological and structural properties of PEDOTh films. *J. Solid State Electrochem.* **2009,** *13* (3), 417-426.
2. Povlich, L. K.; Cho, J. C.; Leach, M. K.; Corey, J. M.; Kim, J.; Martin, D. C., Synthesis, copolymerization and peptide-modification of carboxylic acid-functionalized 3, 4-ethylenedioxythiophene (EDOTacid) for neural electrode interfaces. *Biochimica et Biophysica Acta (BBA)-General Subjects* **2013,** *1830* (9), 4288-4293.
3. Guan, X.-h.; CHEN, G.-h.; Shang, C., ATR-FTIR and XPS study on the structure of complexes formed upon the adsorption of simple organic acids on aluminum hydroxide. *Journal of Environmental Sciences* **2007,** *19* (4), 438-443.
4. Ostrovsky, S.; Hahnewald, S.; Kiran, R.; Mistrik, P.; Hessler, R.; Tscherter, A.; Senn, P.; Kang, J.; Kim, J.; Roccio, M., Conductive hybrid carbon nanotube (CNT)–polythiophene coatings for innovative auditory neuron-multi-electrode array interfacing. *RSC Advances* **2016,** *6* (48), 41714-41723.
5. Nie, T.; Xu, J.-K.; Lu, L.-M.; Zhang, K.-X.; Bai, L.; Wen, Y.-P., Electroactive species-doped poly (3, 4-ethylenedioxythiophene) films: Enhanced sensitivity for electrochemical simultaneous determination of vitamins B2, B6 and C. *Biosens. Bioelectron.* **2013,** *50*, 244-250.
6. Nie, T.; Leng, J.; Bai, L.; Lu, L.; Xu, J.; Zhang, K., Synthesis and characterization of benzenesulfonate derivatives doped poly (3, 4-ethylenedioxythiophene) films and their application in electrocatalysis. *Synth. Met.* **2014,** *189*, 161-172.
7. Kvarnström, C.; Neugebauer, H.; Blomquist, S.; Ahonen, H.; Kankare, J.; Ivaska, A.; Sariciftci, N., In situ FTIR spectroelectrochemical characterization of poly (3, 4-ethylenedioxythiophene) films. *Synth. Met.* **1999,** *101* (1-3), 66.
8. Fabretto, M.; Zuber, K.; Hall, C.; Murphy, P.; Griesser, H. J., The role of water in the synthesis and performance of vapour phase polymerised PEDOT electrochromic devices. *J. Mater. Chem.* **2009,** *19* (42), 7871-7878.
9. Aradilla, D.; Azambuja, D.; Estrany, F.; Iribarren, J. I.; Ferreira, C. A.; Alemán, C., Poly (3, 4-ethylenedioxythiophene) on self-assembled alkanethiol monolayers for corrosion protection. *Polymer Chemistry* **2011,** *2* (11), 2548-2556.
10. Spanninga, S. A.; Martin, D. C.; Chen, Z., X-ray photoelectron spectroscopy study of counterion incorporation in poly (3, 4-ethylenedioxythiophene). *The Journal of Physical Chemistry C* **2009,** *113* (14), 5585-5592.
11. Sappia, L. D.; Piccinini, E.; Marmisollé, W.; Santilli, N.; Maza, E.; Moya, S.; Battaglini, F.; Madrid, R. E.; Azzaroni, O., Integration of biorecognition elements on PEDOT platforms through supramolecular interactions. *Advanced Materials Interfaces* **2017,** *4* (17), 1700502.
12. Wannapob, R.; Vagin, M. Y.; Liu, Y.; Thavarungkul, P.; Kanatharana, P.; Turner, A. P.; Mak, W. C., Printable Heterostructured Bioelectronic Interfaces with Enhanced Electrode Reaction Kinetics by Intermicroparticle Network. *ACS applied materials & interfaces* **2017,** *9* (38), 33368-33376.
13. Peik-See, T.; Pandikumar, A.; Nay-Ming, H.; Hong-Ngee, L.; Sulaiman, Y., Simultaneous electrochemical detection of dopamine and ascorbic acid using an iron oxide/reduced graphene oxide modified glassy carbon electrode. *Sensors* **2014,** *14* (8), 15227-15243.

14. Atta, N. F.; Galal, A.; Ahmed, R. A., Voltammetric behavior and determination of isoniazid using PEDOT electrode in presence of surface active agents. *Int. J. Electrochem. Sci* **2011,** *6* (10), 5097-5113.
15. Xu, G.; Li, B.; Cui, X. T.; Ling, L.; Luo, X., Electrodeposited conducting polymer PEDOT doped with pure carbon nanotubes for the detection of dopamine in the presence of ascorbic acid. *Sensors and Actuators B: Chemical* **2013,** *188*, 405-410.
16. Sheng, G.; Xu, G.; Xu, S.; Wang, S.; Luo, X., Cost-effective preparation and sensing application of conducting polymer PEDOT/ionic liquid nanocomposite with excellent electrochemical properties. *RSC Advances* **2015,** *5* (27), 20741-20746.
17. Harish, S.; Mathiyarasu, J.; Phani, K.; Yegnaraman, V., PEDOT/palladium composite material: synthesis, characterization and application to simultaneous determination of dopamine and uric acid. *J. Appl. Electrochem.* **2008,** *38* (11), 1583-1588.
18. Choe, J. E.; Ahmed, M. S.; Jeon, S., Trouble free dopamine sensing by palladium nanoparticles fabricated poly (3, 4-ethylenedioxythiophene) functionalized graphene. *J. Electrochem. Soc.* **2016,** *163* (3), B113-B118.
19. Yu, S.; Luo, C.; Wang, L.; Peng, H.; Zhu, Z., Poly (3, 4-ethylenedioxythiophene)-modified Ni/silicon microchannel plate electrode for the simultaneous determination of ascorbic acid, dopamine and uric acid. *Analyst* **2013,** *138* (4), 1149-1155.
20. Atta, N. F.; Galal, A.; Ali, S. M.; El-Said, D. M., Improved host–guest electrochemical sensing of dopamine in the presence of ascorbic and uric acids in a β-cyclodextrin/Nafion®/polymer nanocomposite. *Analytical Methods* **2014,** *6* (15), 5962-5971.
21. Atta, N. F.; Galal, A.; Ahmed, R. A., Poly (3, 4-ethylene-dioxythiophene) electrode for the selective determination of dopamine in presence of sodium dodecyl sulfate. *Bioelectrochemistry* **2011,** *80* (2), 132-141.

2019-08-26

Modulating Electrode Kinetics for Discrimination of Dopamine by a PEDOT:COOH Interface Doped with Negatively Charged Tricarboxylate

Meng, Lingyin

American Chemical Society

Meng L, Turner APF, Mak WC. (2019) Modulating Electrode Kinetics for Discrimination of Dopamine by a PEDOT:COOH Interface Doped with Negatively Charged Tricarboxylate. ACS Applied Materials and Interfaces, Volume 11, Issue 37, 2019, pp. 34497-34506

https://doi.org/10.1021/acsami.9b12946